N-Donor Functionalized Acetylacetones for Heterobimetallic CPs, the Next Episode: Trimethylpyrazoles

Steven van Terwingen,[†] Noah Nachtigall,[†] Ben Ebel,[†] and Ulli Englert[*,†,‡]

[†]*RWTH Aachen University, Institute of Inorganic Chemistry, Aachen, Germany*

[‡]*Shanxi University, Key Laboratory of Materials for Energy Conversion and Storage, Institute of Molecular Science, Taiyuan, Shanxi 030006, People's Republic of China*

E-mail: ullrich.englert@ac.rwth-aachen.de

Abstract

The ditopic molecule 3-(1,3,5-trimethyl-4-1*H*-pyrazolyl)acetylacetone (HacacMePz) combines an acetylacetone group suitable for deprotonation and O,O' coordination to a Pearson-hard cation with a softer N-donor site. Both binding modes were employed individually: The pyrazolyl moiety was coordinated to Zn^{II}, Cd^{II}, Hg^{II} and Ag^{I}, and with trivalent iron the tris-chelating O,O' complex [Fe(acacMePz)$_3$] was isolated. The Cu^{II} derivative shows shorter O,O' chelation and N coordination in the more distant Jahn-Teller sites and exists in two alternative crystal forms, namely as a tetranuclear discrete complex and as a chain polymer. The different Pearson hardnesses of the coordination sites of acacMePz$^-$ allow for the design of well-ordered mixed-metal solids. Selective complexation to a hard and a soft cation was achieved in coordination polymers combining hard Fe^{III} and softer Hg^{II} or Ag^{I}. Even slight differences in Pearson hardness based on different oxidation states of the same cation imply sufficient selectivity, as shown by the successful synthesis of a mixed-valent Cu^{II}/Cu^{I} chain polymer. A

synopsis of all structurally characterized compounds confirms that HacacMePz represents a bridging ligand with restricted conformational freedom. No full rotation about the single bond between the pyrazolyl and acetylacetone fragments occurs, and dihedral angles between these moieties are limited to values of $90° \pm 17°$.

Introduction

Over the last decades coordination polymers (CPs) have attracted increasing interest in various fields of research[1–5] due to their applications in catalysis,[6–8] gas storage and separation[9,10] and optical properties.[11–13] They can combine high porosity and stability[14,15] which enables their relevance for industrial processes and competition with industry-standards such as zeolites.[16–18] Since CPs can incorporate a broad variety of elements and take advantage of element-specific properties, e. g. luminescence of lanthanides,[19,20] it is advantageous to combine two or more different metal cations in a single CP. However, only a small fraction of all reported CPs incorporate two or more metal species. A quick search in SciFinder^n reveals that only approximately 1 % of articles published regarding CPs cover heterobimetallic species.[§] This is predominantly due to their more elaborate synthesis compared to monometallic CPs: The necessity of selectivity towards specific metal cations narrows down the scope of suitable ligands massively.

Utilizing heterobifunctional ditopic ligands with different coordination sites regarding their Pearson hardness can accomplish this crucial selectivity.[21] Due to their convenient and predictable coordination chemistry acetylacetones are promising scaffolds for the rational design of such ligands.[22,23] Early work by Chen et al.[24] and Vreshch et al.[25] for pyridyl (HacacPy) and by Burrows et al.[26] and Kondracka et al.[27] for nitrile (HacacCN) substituted acetylacetones have proven suitable for this purpose (Figure 1).

[§]Results for "bimetallic" and "coordination polymer": 449 vs. search for "coordination polymer" only: 33384. Performed on 29.01.21.

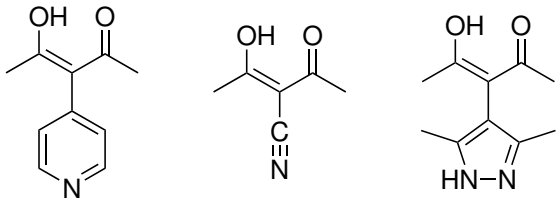

Figure 1: Ditopic N-donor substituted acetylacetones for the preparation of heterobimetallic CPs: 3-(4-pyridyl)acetylacetone,[25] 3-cyanoacetylacetone,[26,27] and 3-(3,5-dimethyl-4-1*H*-pyrazolyl)acetylacetone.[28]

In 2016, we could demonstrate that a heterogenous solid with Ag^0 nanoparticles on Yb_2O_3 derived from thermal decomposition of a CP of HacacCN with Yb^{III}/Ag^{I} is more active for the N_2O decomposition than a catalyst synthesized by precipitation and subsequent calcination.[29] Upscaling of the syntheses proved to be challenging and time consuming. A more accessible ligand with a pyrazolyl substituent (H_2acacPz) was introduced in the same year, but has not yet been applied as a catalyst precursor.[28,30] Although its synthesis and coordination chemistry proved to be straightforward, the second acidic proton at the pyrazolyl group introduced further complexity to the system. We addressed this issue by substituting the acidic N–H proton for a methyl group and obtained the target ligand for this contribution: (3-(1,3,5-trimethyl-4-1*H*-pyrazolyl)acetylacetone (HacacMePz) (**1**). Although alternative orientations for this extra methyl group might be encountered for uncoordinated pyrazolyl moieties, this potential disorder should obviously be irrelevant in our mixed-metal target solids.

Results and Discussion

In Scheme 1 an overview of all compounds presented in this work is given. Both selective N and O coordination were achieved. In addition to exclusive N and O coordination, we were able to obtain two mixed-metal CPs: a heterobimetallic CP with Fe^{III}/Hg^{II} and a mixed valence CP with Cu^{II}/Cu^{I}.

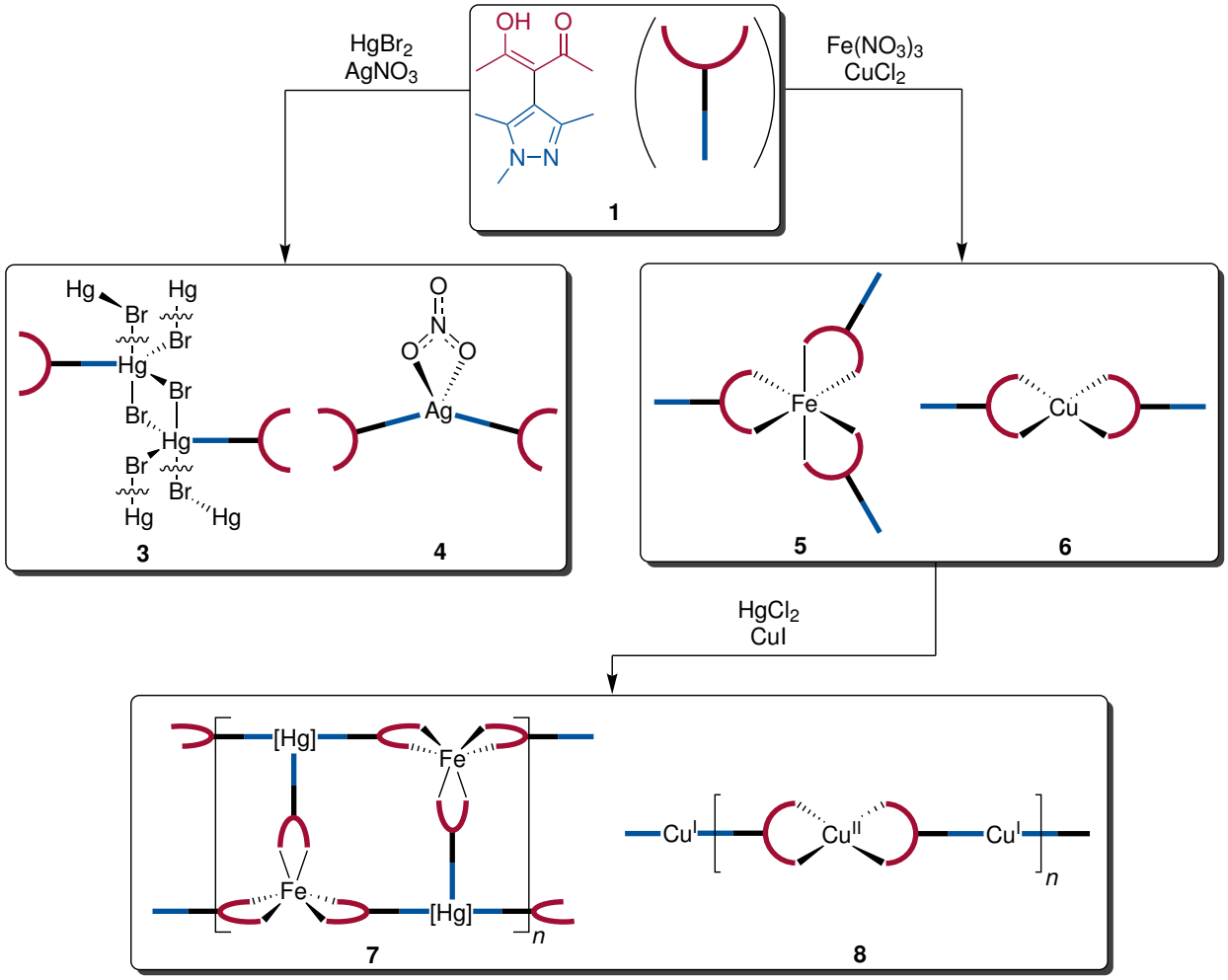

Scheme 1: Schematic overview of the compounds presented in this work. HacacMePz (**1**) has been simplified in the coordination compounds for clarity. [Hg] denotes a $\{Hg_2Cl_4\}$ secondary building unit.

Synthesis and Crystal Structures of the Uncoordinated Ligand

HacacMePz (**1**) is synthesized from the readily available tetraacetylethane (TAE).[31,32] Afterwards methylhydrazine is used to form the desired trimethylpyrazole and two equivalents of water. Since this reaction does not prefer a specific site of the bis-β-diketone, it affords 50 % HacacMePz, while the other half of bis-β-diketone either does not react at all or undergoes condensation with two equivalents of methylhydrazine (Scheme 2).

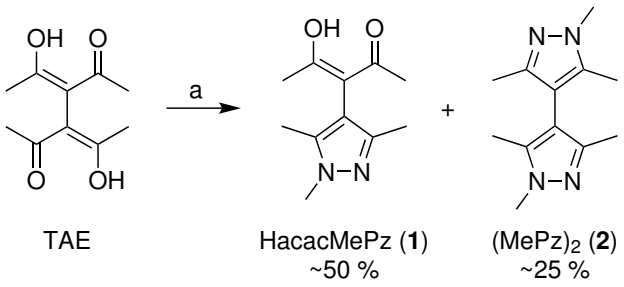

Scheme 2: Synthetic procedure to obtain HacacMePz (**1**) and the expected yields. Twofold substitution leads to the undesired bis-pyrazole $(\mathrm{MePz})_2$ (**2**). Reaction conditions a: 1 eq. hydrazine, abs. ethanol, 4 h reflux.

The three compounds differ significantly with respect to solubility and may therefore be rather easily separated by crystallization. Recovered TAE may be recycled in a subsequent ligand synthesis (section S1). The expected yield of 50 % per batch can thus be substantially increased by reusing the recovered TAE to a theoretical maximum yield of 67 % using one equivalent of methylhydrazine. We found several modifications of HacacMePz and will discuss one of them here in the main text. Form **1**α of the ligand crystallizes in the orthorhombic space group *Pbca* with $Z = 8$. Like most acetylacetones with one substituent in 3-position it adopts the enol form in both solution and solid state.[33] The enol hydrogen is well ordered within the intramolecular hydrogen bond; it may be located as local density maximum in a difference Fourier map (Figure S1).

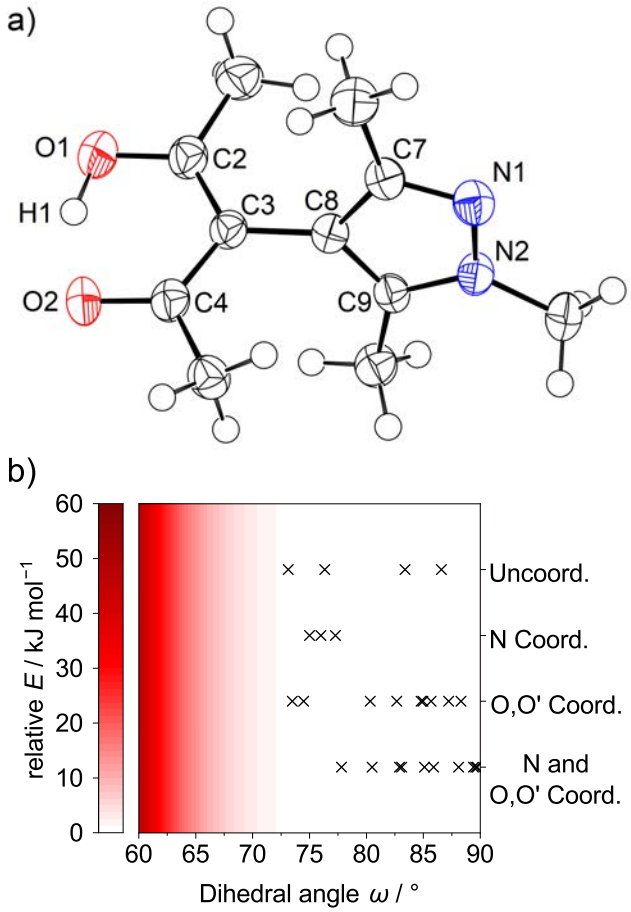

Figure 2: a) ORTEP plot[34] of **1**α drawn at 70 % probability. Selected intramolecular distances and angles (Å, °): O1–C2 1.321(2), O2–C4 1.273(2), C2–C3 1.388(2), C3–C4 1.426(2), H1···O2 1.47(2), ω 73.13(9). b) Distribution for the angle ω subtended by acetylacetone and pyrazole least square planes; the background color encodes the energy profile according to a simplified rigid force field calculation.

The assignment of the H atom is corroborated by the distance pattern between the non-hydrogen atoms in the Hacac moiety: The C–O distances differ by about 0.05 Å; C2–C3 is closer to a C=C double bond, whereas C3–C4 can be described as a rather short C–C single bond. While investigating the coordination chemistry of HacacMePz, we encountered a second polymorph and two hydrates of **1** as well as the disubstituted compound **2**. Crystal structures of **1**β, **1**$\cdot 0.5\,H_2O$, **1**$\cdot 2\,H_2O$ and **2**$\cdot 2\,H_2O$ are compiled in the ESI. For our comparison between the alternative crystal forms of **1** and its derivatives throughout our journey exploring the coordination of HacacMePz, we will make use of the dihedral angle ω subtended by the least squares planes of the acetylacetone (O1, O2, C2, C3, C4) and

pyrazolyl (N1, N2, C7, C8, C9) moieties. In Figure 2b the energy profile of a simplified force field calculation is depicted, together with all individual values for ω encountered in the compounds **1** to **8**. The steric requirements of the acetylacetonato and pyrazolyl methyl groups prevent full rotation about the C3–C8 bond. In view of the inherent mirror symmetry of the acetylacetonato group, we only considered torsion angles $\leq 90°$. All 26 experimental observations for ω, regardless of any additional coordination to the ditopic moiety, adopt values in the range of $90° \pm 17°$ and thus fit into the energetically favorable section of conformational space.

N Coordination Capabilities

While N coordination with nitrile groups as the N-donor, e. g. HacacCN, can be challenging to achieve,[26,27,35–40] HacacMePz's donor capabilities are more reliable. Its reaction with MX_2 (M = Zn, Cd, Hg; X = Cl, Br, I) readily yields N coordinated complexes in each case. The resulting complexes are very similar, and here only the coordination compound of HacacMePz to $HgBr_2$ will be discussed in detail. $[Hg(HacacMePz)(\mu_2\text{-}Br)_2]^2_\infty$ (**3**) crystallizes in the monoclinic space group $P2_1/c$ with $Z = 4$ (Figure 3).

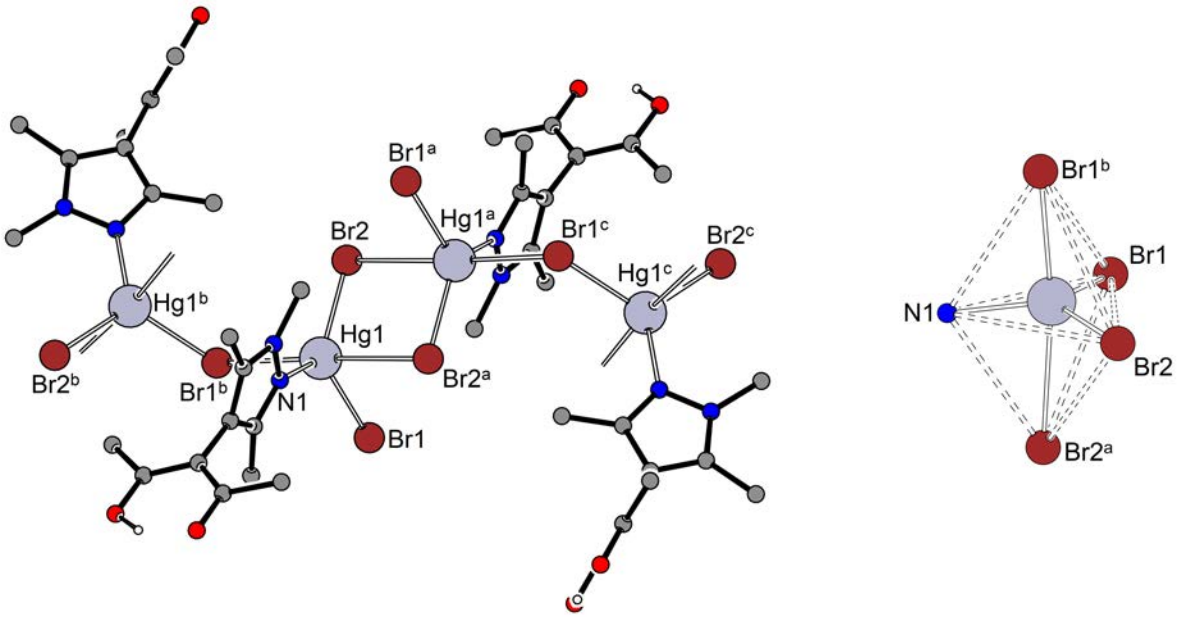

Figure 3: PLUTON plot[34] of an excerpt of the chain structure in **3** (left, C-bonded hydrogen omitted) and the coordination sphere around Hg1 (right). Selected intramolecular distances and angles (Å, °): Hg1–N1 2.212(3), Hg1–Br1 2.5732(6), Hg1–Br2 2.5343(5), Hg1–$Br1^{b}$ 2.9104(5), Hg1–$Br2^{a}$ 3.2849(7), N1–Hg1–Br1 116.70(9), $Br1^{b}$–Hg1–$Br2^{a}$ 172.38(2), ω 76.0(3). Symmetry operators: a $= 1-x, 1-y, 2-z$; b $= 1-x, 0.5+y, 1.5-z$; c $= x, 0.5-y, 0.5+z$.

The mercury(II) ion is coordinated by one HacacMePz and four bromido ligands. The coordination sphere around Hg1 can be described as a distorted trigonal bipyramid ($\tau_5 = 0.82$)[41] with two differently elongated axial positions. The bromido ligand Br2 acts as a strongly asymmetric bridge between two Hg^{II} cations related by crystallographic inversion (Wyckoff position 2*d*), thus forming a $\{Hg_2Br_2\}$ unit. Br1 links neighboring units in a slightly less asymmetric fashion. The resulting two-dimensional polymer extends in the (1 0 0) plane.

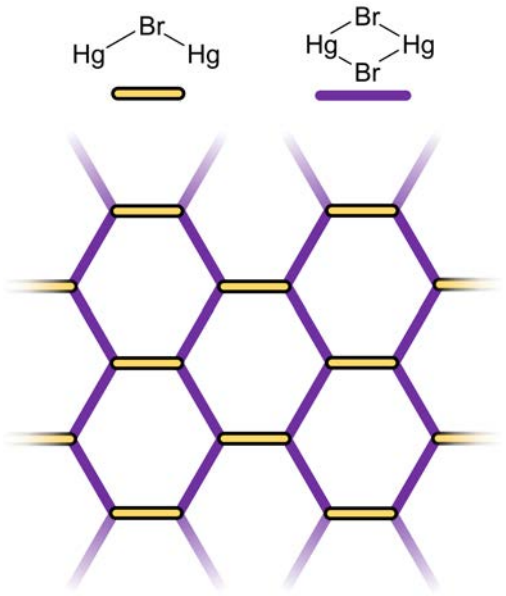

Figure 4: Simplified depiction of the two-dimensional **hcb**-like coordination polymer formed by the Hg^{II} ions and their μ_2 bridging bromido ligands in **3**.

If Hg cations are perceived as nodes and single and double bridged Hg···Hg as equivalent edges, its topology corresponds to the honeycomb (**hcb**) net. If the different edges are treated as non-equivalent as shown in Figure 4, no topology match could be found in the RSCR,[42] but the arrangement resembles one of the limiting mesomeric structures in graphite.

While mercury has interesting properties, e. g. luminescence, it is rather toxic. Other d^{10} cations, e. g. Ag^{I} and Cu^{I}, exhibit similar properties and are frequently used as soft metals for heterobimetallic CPs. Thus, N coordination was also achieved with a variety of Ag^{I} salts. As an example the coordination compound of $AgNO_3$ with HacacMePz will be described here: The resulting mononuclear complex $[Ag(HacacMePz)_2(NO_3)]$ (**4**) crystallizes in the polar monoclinic space group $P2_1$ with $Z = 2$ (Figure 5).

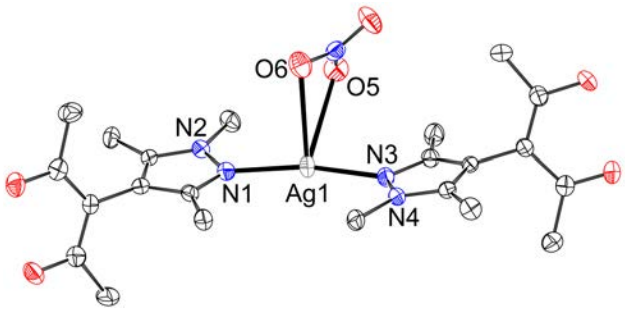

Figure 5: ORTEP plot[34] of **4** drawn at 70 % probability (hydrogen omitted). Selected intramolecular distances and angles (Å, °): Ag1–N1 2.125(2), Ag1–N3 2.135(2), Ag1–O5 2.830(2), Ag1–O6 2.755(2), N1–Ag1–N3 167.21(8), O5–Ag1–O6 45.74(6), ω_1 77.27(16), ω_2 75.00(15).

For cationic bis(pyrazolyl) Ag^I complexes different coordination modes of the nitrate counteranion have been described: NO_3^- can be non-coordinating, mono- or bidentate, and even bridging two $[AgPz_2]^+$ moieties (refcodes ISAHUH,[28] EMAFOO,[43] PAWBEW[44]). In our case, the nitrate ion interacts with the cation in a bidentate fashion with two Ag···O contacts of about 2.8 Å. This interaction with the nitrate leads to a small deviation from a perfectly linear N–Ag–N coordination with an angle of approx. 167°. This geometry prevents local inversion at the Ag^I ion as it is encountered e. g. in ISAHUH. Both acetylacetone moieties adopt the enol tautomer; while ligand 1 shows a disordered enol hydrogen, in agreement with C–O bonds of very similar length, ligand 2 features a well-localized H atom in the intramolecular O–H···O bond and a difference of approx. 0.06 Å between single and double C–O bonds.

O,O' Coordination

O,O' chelation of the ligand to a Pearson-hard metal cation requires deprotonation of the acetylacetone moiety prior to coordination and, hence, more harsh reaction conditions. The deprotonation can be achieved by adding an external base or by using a basic metal salt. In contrast to the uniquely defined N coordination, O,O' coordination of HacacMePz leads to a mixture of isomers. For square-planar $[M(acacMePz)_2]$ *cis*/*trans* isomerism is encountered

(Scheme 3), and in pseudo-octahedral [M(acacMePz)$_3$] complexes a total of four rather than the usual two helical Δ/Λ isomers may occur.

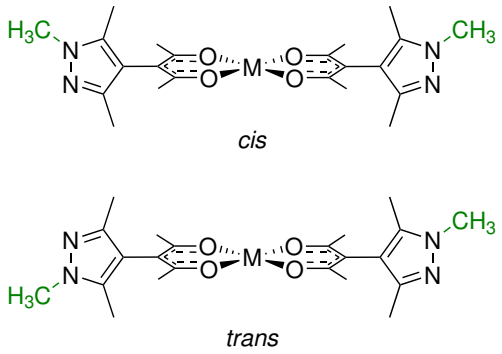

Scheme 3: The two different isomers arising from the O,O' square planar coordination of two acacMePz$^-$ moieties to a metal ion M.

Upon crosslinking, different isomers of inert metal cations could easily result in hardly tractable mixtures of coordination polymers. Therefore, we focused on complexes of metal cations with coordination spheres that allow ligand exchange on a reasonable time scale. Reaction of HacacMePz with Fe(NO$_3$)$_3$ leads to the tris-acetylacetonato complex [Fe(acacMePz)$_3$] (**5**). The compound crystallizes as a hydrate in the triclinic space group $P\bar{1}$ with $Z = 2$.

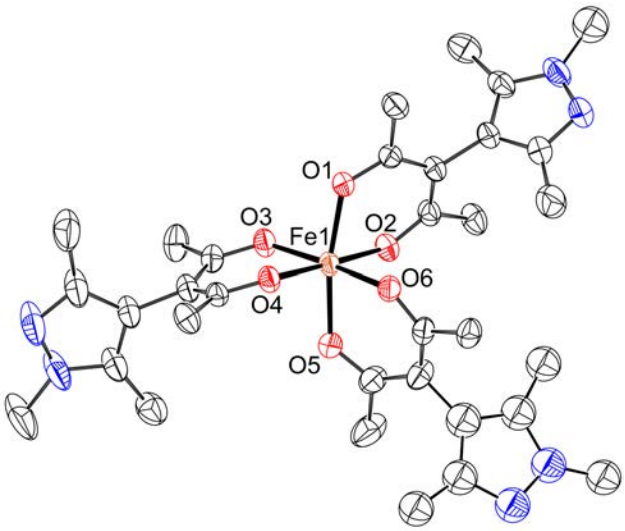

Figure 6: Displacement ellipsoid plot[34] of **5** · 8.3 H_2O (70 % probability, minority component in a disordered ligand and water molecules omitted). Selected intramolecular distances and angles (Å, °): Fe1–O1 1.9806(19), Fe1–O6 2.0050(18), ω_1 84.97(11), ω_2 82.66(12), ω_3 74.48(15).

The acetylacetonate oxygen atoms form a nearly regular octahedron around Fe1. Instead of one specific isomer, all isomers cocrystallize in the same solid, albeit with different occupancies. The superposition of different isomers in the crystal results in disorder for methyl substituents at the alternative pyrazole N atoms. Water molecules act as hydrogen bond donors to the free pyrazole nitrogen atoms. Further details concerning this coupled disorder and the orientational disorder of a complete acacMePz$^-$ ligand are available in the ESI and the associated CIF.

Another candidate for O,O' coordination is Cu^{II}. Typically Jahn-Teller distorted Cu^{II} features a square planar equatorial coordination and up to two usually more remote axial positions which may be coordinated by soft donors, e. g. the pyrazole N. We found two phases of the resulting compound $[Cu(acacMePz)_2]_n$ (**6**) with equal repeating units but different connectivity between them.

Both phases form upon reaction of HacacMePz with $CuCl_2$ and a base. The discrete complex $[Cu(acacMePz)_2]_4$ (**6**α) crystallizes as a dihydrate in the triclinic space group $P\bar{1}$ with $Z = 1$ (Figure 7); the asymmetric unit contains two Cu^{II} cations. Both cations adopt square pyramidal coordination, with τ_5 values of 0.05 for Cu1 and 0.36 for Cu2.[41] Each center is coordinated by two acetylacetonato ligands in the basal plane and a pyrazole nitrogen in the apical position. A similar tetranuclear Cu^{II} complex was observed by Tong et al. with H_2acacPz.[30]

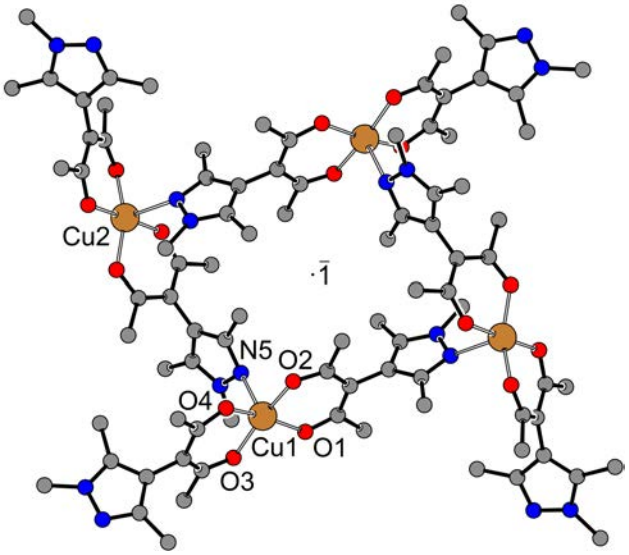

Figure 7: PLUTON plot[34] of **6**α · 2 H_2O (hydrogen, water molecules and minority component omitted). Selected intramolecular distances and angles (Å, °): Cu1–O1 1.937(2), Cu1–O2 1.908(2), Cu1–O3 1.920(2), Cu1–O4 1.934(2), Cu1–N4 2.382(3), ω_2 73.48(18), ω_3 87.22(19).

$[Cu(acacMePz)_2]^1_\infty$ (**6**β) crystallizes in the monoclinic space group $P2_1/n$ with $Z = 4$ and corresponds to a one-dimensional chain polymer. The asymmetric unit comprises a single $[Cu(acacMePz)_2]$ moiety. The Cu^{II} cation is coordinated in a square pyramidal fashion with $\tau_5 = 0.15$. One of the two pyrazole rings of the $[Cu(acacMePz)_2]$ moiety is coordinated to the apical position of an adjacent Cu^{II} complex generated by the glide plane along [1 0 1] (Figure 8). The one-dimensional chains propagate along [1 0 –1]. The $acacMePz^-$ moiety with the uncoordinated pyrazolyl substituent shows disorder; refinement of the alternative N-methyl sites associated with N3 and N4 converged for a 80.9(7) % site occupancy of the majority conformer.

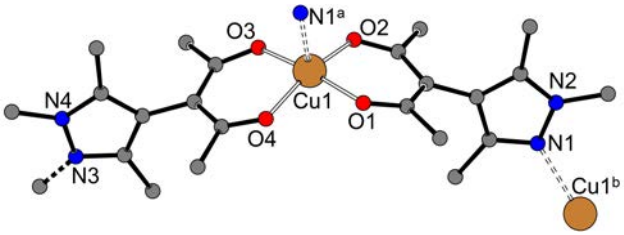

Figure 8: PLUTON plot[34] of the asymmetric residue of **6**β (hydrogen omitted, disordered methyl on N3). Selected intramolecular distances and angles (Å, °): Cu1–O1 1.9300(18), Cu1–O2 1.9377(16), Cu1–O3 1.9319(17), Cu1–O4 1.9400(17), Cu1–N1^{a} 2.2940(19), ω_1 88.3(3), ω_2 84.8(3). Symmetry operators: a $= -0.5 + x, 1.5 - y, 0.5 + z$; b $= 0.5 + x, 1.5 - y, -0.5 + z$.

Both crystal forms of [Cu(acacMePz)$_2$] precipitate concomitantly; the powder pattern (Figure S10) is clearly dominated by the chain polymer **6**β. We have not been able to trigger preferential formation of **6**α by seeding.

Selective Ditopic Coordination of HacacMePz

We have shown above that both binding sites of HacacMePz may reliably be used for metal coordination. The heterobimetallic target compounds are usually synthesized via initial O,O' coordination and subsequent crosslinking via the softer N site, because the former requires harsher reaction conditions. Reaction of **5** with $HgCl_2$ leads to the formation of the heterobimetallic one-dimensional chain polymer $[Fe(acacMePz)_3Hg(\mu_2\text{-}Cl)ClHgCl_2]^1_\infty$ (**7**). It crystallizes as an acetonitrile solvate in the triclinic spacegroup $P\bar{1}$ with $Z = 2$ (Figure 9).

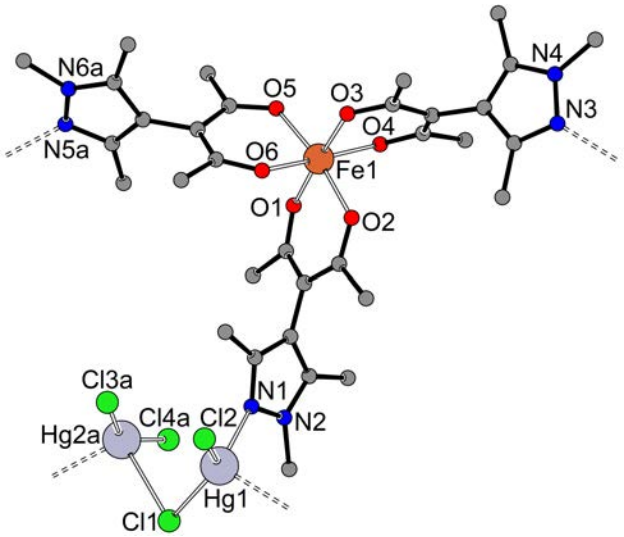

Figure 9: PLUTON plot[34] of the asymmetric residue of $\mathbf{7} \cdot 1.5\,\mathrm{MeCN}$ (hydrogen atoms, solvent MeCN and minority component omitted). Selected intramolecular distances and angles (Å, °): Hg1–N1 2.285(10), Hg1–Cl1 2.446(4), Hg1–Cl2 2.389(4), Hg2a–Cl1 2.773(5), Fe1–O1 1.977(9), ω_1 88.3(3), ω_2 84.8(3).

The coordination sphere of the Fe^{III} ion is a rather regular octahedron; the Hg^{II} ions adopt distorted tetrahedral coordination environments ($\tau_4 = 0.82$ and 0.76).[41] One chloride acts as a μ_2 bridging ligand whereas the other three are monovalent bound to their respective Hg^{II} ion. This connectivity leads to a one-dimensional ladder-like coordination polymer which expands in [1−1 1] direction. The strands do not show any meaningful interactions between adjacent chains.

Both the +I and the +II oxidation states are well known for copper. We achieved the selective formation of a mixed valence Cu^{II}/Cu^{I} CP with HacacMePz where both oxidation states coexist in the same solid. This confirms the selectivity of HacacMePz towards hard and soft metal ions. The compound $[Cu(acacMePz)_2(MeCN)_2CuI]^1_\infty$ ($\mathbf{8} \cdot 2\,\mathrm{MeCN}$) crystallizes in the monoclinic space group $C2/c$ with $Z = 4$ (Figure 10).

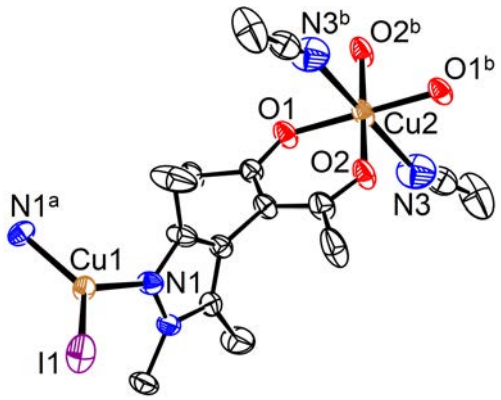

Figure 10: Displacement ellipsoid plot[34] of $\mathbf{8} \cdot 2\,\mathrm{MeCN}$ (70 % probability, hydrogen omitted). Selected intramolecular distances and angles (Å, °): Cu1–N1 1.9911(18), Cu2–O1 1.9337(15), Cu2–N3 2.743(2), N1–Cu1–N1^{a} 109.56(11), N1–Cu1–I1 125.22(6), ω 89.74(12). Symmetry operators: a $= 1-x, y, 0.5-z$; b $= 1-x, 2-y, 1-z$.

Both copper ions occupy special positions: Cu1 and its coordinated iodido ligand are located on the twofold rotation axis at Wyckoff position 4*e*, and Cu2 is located on an inversion center at Wyckoff position 4*b*. The coordination geometries around Cu1 and Cu2 are rather regular. The monovalent Cu1 adopts a trigonal planar coordination involving the iodide anion and two pyrazolyl N-donors of acacMePz^{-} ligands. The divalent Cu2 has a distorted octahedral coordination sphere. Bond valence considerations confirm our assignment of the different oxidation states, with valence sums of 0.93 for Cu1 and 2.06 for Cu2.[45,46] The equatorial coordination sites are occupied by two acetylacetonate moieties. Two presumably weakly bonded acetonitrile molecules complete the Jahn-Teller elongated coordination sphere in the axial positions. The resulting one dimensional CP expands along [0 0 1] in a "zig-zag" arrangement.

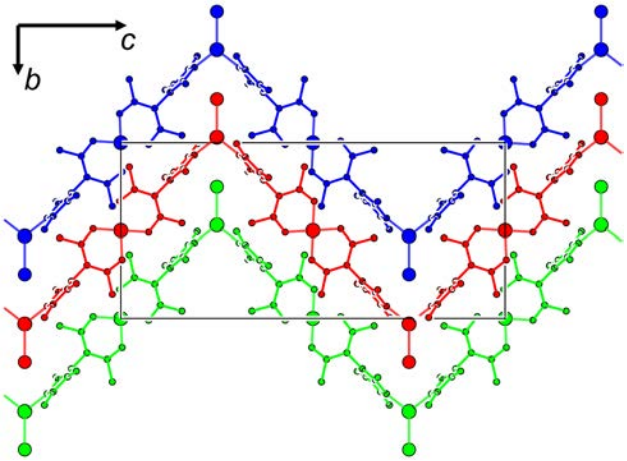

Figure 11: PLUTON plot[34] of three chains in $\mathbf{8} \cdot 2\,\mathrm{MeCN}$ depicted in three different colors (hydrogen and solvent MeCN molecules omitted).

When a microcrystalline bulk sample is removed from the mother liquor, immediate desolvation occurs, accompanied by a color change from cyan to green within seconds. When acetonitrile is re-introduced into the system, the color changes back to the original cyan, and we propose this color change is associated with a change in the coordination sphere of the divalent copper cations. Desolvation is slower and requires minutes for larger single crystals of $\mathbf{8} \cdot 2\,\mathrm{MeCN}$. Unfortunately, we have not been able to index the diffraction pattern of the desolvation product and obtain structural information at atomic resolution. To prove our assumption we performed powder XRD of a dry and a wet sample and compared it to the simulated powder pattern from the single crystal XRD (Figure S12). Furthermore, the characteristic IR band of the C≡N deformation is not observed in the dried sample.

Conclusion

In this contribution we advocate the use of a methyl- rather than an unsubstituted pyrazolyl N-donor substituent in order to avoid any deprotonation ambiguity. This aim has been achieved with 3-(1,3,5-trimethyl-4-1*H*-pyrazolyl)acetylacetone HacacMePz, but with respect to the O,O' coordinated intermediate [Fe(acacMePz)$_3$], this happens at the expense of conformational disorder. Such disorder is tolerated in the dicrete mononuclear and sol-

vated building block, but as anticipated in our original design idea for HacacMePz, it is not retained in the heterometallic target solids. The intermediate Fe^{III} complex is sufficiently labile to undergo configurational changes, and the inherent trend to efficient space filling favors the formation of quite well-ordered extended structures upon crosslinking with soft cations. HacacMePz proves well-suited for crystal engineering: In all 26 structurally characterized occurences of the molecule or its derivatives, the acetylacetone and the pyrazolyl moieties show an almost orthogonal arrangement; only a small part of conformational space, corresponding to dihedral angles of $90° \pm 17°$ (Figure 2b), is populated. Future work will focus on O,O' coordination to rare earth cations and crosslinking of the dangling N-donor sites by soft cations.

Acknowledgement

We thank Dr. Carsten Paulmann for his help with the diffraction experiment performed at PETRA-III, DESY. An RWTH fellowship to SvT is gratefully acknowledged. UE acknowledges support from the One Hundred-Talent Program of Shanxi Province.

Supporting Information Available

Experimental section, details on X-ray diffraction data processing and crystal data refinement, powder XRD data, NMR spectra of **1** and **2** and pictures of $\mathbf{6}\alpha \cdot 2\,H_2O$ and $\mathbf{6} \cdot 2\,MeCN$.

References

(1) Tran, M.; Kline, K.; Qin, Y.; Shen, Y.; Green, M. D.; Tongay, S. 2D coordination polymers: Design guidelines and materials perspective. *Appl. Phys. Rev.* **2019**, *6*, 041311.

(2) Bureekaew, S.; Shimomura, S.; Kitagawa, S. Chemistry and application of flexible porous coordination polymers. *Sci. Technol. Adv. Mater.* **2008**, *9*, 014108.

(3) Kitagawa, S.; Kitaura, R.; Noro, S.-i. Functional porous coordination polymers. *Angew. Chem. Int. Ed.* **2004**, *43*, 2334–2375.

(4) Ma, M.; Lu, L.; Li, H.; Xiong, Y.; Dong, F. Functional Metal Organic Framework/SiO_2 Nanocomposites: From Versatile Synthesis to Advanced Applications. *Polymers* **2019**, *11*.

(5) Batten, S. R.; Neville, S. M.; Turner, D. R. *Coordination Polymers: Design, Analysis and Application*; RSC Publishing: Cambridge, 2009.

(6) Bansal, D.; Pandey, S.; Hundal, G.; Gupta, R. Heterometallic coordination polymers: syntheses, structures and heterogeneous catalytic applications. *New J. Chem.* **2015**, *39*, 9772–9781.

(7) Chen, Y.; Tang, M.; Wu, Y.; Su, X.; Li, X.; Xu, S.; Zhuo, S.; Ma, J.; Yuan, D.; Wang, C.; Hu, W. A One-Dimensional π-d Conjugated Coordination Polymer for Sodium Storage with Catalytic Activity in Negishi Coupling. *Angew. Chem. Int. Ed.* **2019**, *58*, 14731–14739.

(8) Tang, L.-P.; Yang, S.; Liu, D.; Wang, C.; Ge, Y.; Tang, L.-M.; Zhou, R.-L.; Zhang, H. Two-dimensional porous coordination polymers and nano-composites for electrocatalysis and electrically conductive applications. *J. Mater. Chem. A* **2020**, *8*, 14356–14383.

(9) Koh, K.; Wong-Foy, A. G.; Matzger, A. J. A porous coordination copolymer with over 5000 m^2/g BET surface area. *J. Am. Chem. Soc.* **2009**, *131*, 4184–4185.

(10) Song, K. S.; Kim, D.; Polychronopoulou, K.; Coskun, A. Synthesis of Highly Porous Coordination Polymers with Open Metal Sites for Enhanced Gas Uptake and Separation. *ACS Appl. Mater. Interfaces* **2016**, *8*, 26860–26867.

(11) Almotawa, R. M.; Aljomaih, G.; Trujillo, D. V.; Nesterov, V. N.; Rawashdeh-Omary, M. A. New Coordination Polymers of Copper(I) and Silver(I) with Pyrazine

and Piperazine: A Step Toward Green Chemistry and Optoelectronic Applications. *Inorg. Chem.* **2018**, *57*, 9962–9976.

(12) Visconti, M.; Maggini, S.; Ciani, G.; Mercandelli, P.; Del Secco, B.; Prodi, L.; Sgarzi, M.; Zaccheroni, N.; Carlucci, L. New Lanthanide Metalloligands and Their Use for the Assembly of Ln–Ag Bimetallic Coordination Frameworks: Stepwise Modular Synthesis, Structural Characterization, and Optical Properties. *Cryst. Growth Des.* **2019**, *19*, 5376–5389.

(13) Zhang, T.; Guo, X.; Shi, Y.; He, C.; Duan, C. Dye-incorporated coordination polymers for direct photocatalytic trifluoromethylation of aromatics at metabolically susceptible positions. *Nat. Commun.* **2018**, *9*, 4024.

(14) Rao, K. P.; Higuchi, M.; Suryachandram, J.; Kitagawa, S. Temperature-Stable Compelled Composite Superhydrophobic Porous Coordination Polymers Achieved via an Unattainable de Novo Synthetic Method. *J. Am. Chem. Soc.* **2018**, *140*, 13786–13792.

(15) Akiyama, G.; Matsuda, R.; Kitagawa, S. Highly Porous and Stable Coordination Polymers as Water Sorption Materials. *Chem. Lett.* **2010**, *39*, 360–361.

(16) Peralta, D.; Chaplais, G.; Simon-Masseron, A.; Barthelet, K.; Chizallet, C.; Quoineaud, A.-A.; Pirngruber, G. D. Comparison of the Behavior of Metal-Organic Frameworks and Zeolites for Hydrocarbon Separations. *J. Am. Chem. Soc.* **2012**, *134*, 8115–8126.

(17) Rangnekar, N.; Mittal, N.; Elyassi, B.; Caro, J.; Tsapatsis, M. Zeolite membranes - a review and comparison with MOFs. *Chem. Soc. Rev.* **2015**, *44*, 7128–7154.

(18) Tatlier, M. Performances of MOF vs. zeolite coatings in adsorption cooling applications. *Appl. Therm. Eng.* **2017**, *113*, 290–297.

(19) Huang, P.; Wu, F.; Mao, L. Target-Triggered Switching on and off the Luminescence of Lanthanide Coordination Polymer Nanoparticles for Selective and Sensitive Sensing of Copper Ions in Rat Brain. *Anal. Chem.* **2015**, *87*, 6834–6841.

(20) Xu, C.; Huang, H.; Ma, J.; Liu, W.; Chen, C.; Huang, X.; Yang, L.; Pan, F.-X.; Liu, W. Lanthanide(III) coordination polymers for luminescence detection of Fe(III) and picric acid. *New J. Chem.* **2018**, *42*, 15306–15310.

(21) Pearson, R. G. Hard and soft acids and bases, HSAB, part 1: Fundamental principles. *J. Chem. Edu.* **1968**, *45*, 581–587.

(22) Kremer, M.; Englert, U. N Donor substituted acetylacetones – versatile ditopic ligands. *Z. Kristallogr. – Cryst. Mater.* **2018**, *233*, 437–452.

(23) Gildenast, H.; Nölke, S.; Englert, U. 3-(4-Methylthiophenyl)acetylacetone – ups and downs of flexibility in the synthesis of mixed metal–organic frameworks. Ditopic bridging of hard and soft cations and site-specific desolvation. *CrystEngComm* **2020**, *22*, 1041–1049.

(24) Chen, B.; Fronczek, F. R.; Maverick, A. W. Porous Cu-Cd mixed-metal-organic frameworks constructed from $Cu(Pyac)_2$ Bis[3-(4-pyridyl)pentane-2,4-dionato]copper(II). *Inorg. Chem.* **2004**, *43*, 8209–8211.

(25) Vreshch, V. D.; Chernega, A. N.; Howard, J. A. K.; Sieler, J.; Domasevitch, K. V. Two-step construction of molecular and polymeric mixed-metal Cu(Co)/Be complexes employing functionality of a pyridyl substituted acetylacetonate. *Dalton Trans.* **2003**, 1707–1711.

(26) Burrows, A. D.; Cassar, K.; Mahon, M. F.; Warren, J. E. The stepwise formation of mixed-metal coordination networks using complexes of 3-cyanoacetylacetonate. *Dalton Trans.* **2007**, 2499–2509.

(27) Kondracka, M.; Englert, U. Bimetallic coordination polymers via combination of substitution-inert building blocks and labile connectors. *Inorg. Chem.* **2008**, *47*, 10246–10257.

(28) Guo, Q.; Englert, U. An Acetylacetonate or a Pyrazole? Both! 3-(3,5-Dimethyl-pyrazol-4-yl)pentane-2,4-dione as a Ditopic Ligand. *Cryst. Growth Des.* **2016**, *16*, 5127–5135.

(29) Konkol, M.; Kondracka, M.; Kowalik, P.; Próchniak, W.; Michalska, K.; Schwedt, A.; Merkens, C.; Englert, U. Decomposition of the mixed-metal coordination polymer—A preparation route of the active Ag/Yb_2O_3 catalyst for the deN_2O process. *Appl. Catal., B* **2016**, *190*, 85–92.

(30) Tong, J.; Jia, L.-M.; Shang, P.; Yu, S.-Y. Controlled Synthesis of Supramolecular Architectures of Homo- and Heterometallic Complexes by Programmable Self-Assembly. *Cryst. Growth Des.* **2019**, *19*, 30–39.

(31) Mosby, W. L. The Reactions of Some 1:4-Dicarbonyl Systems with Hydrazine. *J. Chem. Soc.* **1957**, 3997–4003.

(32) Ponomarova, V. V.; Komarchuk, V. V.; Boldog, I.; Krautscheid, H.; Domasevitch, K. V. Modular construction of 3D coordination frameworks incorporating SiF_6^{2-} links: Accessing the significance of [M(pyrazole)$_4$SiF$_6$] synthon. *CrystEngComm* **2013**, *15*, 8280.

(33) Truong, K. N.; Meven, M.; Englert, U. Proton disorder in a short intramolecular hydrogen bond investigated by single-crystal neutron diffraction at 2.5 and 170 K. *Acta Crystallogr.* **2018**, *C74*, 1635–1640.

(34) Spek, A. L. Structure validation in chemical crystallography. *Acta Crystallogr.* **2009**, *D65*, 148–155.

(35) Balahura, R. J.; Ferguson, G.; Johnston, A.; Ruhl, B. L. Reactions and X-Ray Crys-

tal Structure of (3-Cyano-2,4-pentanedionato-N)pentaamminecobalt(III) Perchlorate Chloride Dihydrate. *Polyhedron* **1986**, *5*, 2075–2080.

(36) Tsiamis, C.; Tzavellas, L.; Stergiou, A.; Anesti, V. Variable Coordination and Conformation of the 3-Cyano-2,4-pentanedionato Anion in a Mixed-Ligand Binuclear Copper(II) Chelate. *Inorg. Chem.* **1996**, *35*, 4984–4988.

(37) Pogozhev, D.; Baudron, S. A.; Hosseini, M. W. Assembly of heteroleptic copper complexes with silver salts: from discrete trinuclear complexes to infinite networks. *Inorg. Chem.* **2010**, *49*, 331–338.

(38) Merkens, C.; Becker, N.; Lamberts, K.; Englert, U. Bimetallic coordination networks based on Al(acacCN)$_3$: a building block between inertness and lability. *Dalton Trans.* **2012**, *41*, 8594–8599.

(39) Merkens, C.; Englert, U. Ordered bimetallic coordination networks featuring rare earth and silver cations. *Dalton Trans.* **2012**, *41*, 4664–4673.

(40) Guo, Q.; Englert, U. Neutral mixed-metal coordination polymers based on a ditopic acetylacetonate, Mg(II) and Ag(I): syntheses, characterization and solvent-dependent topologies. *Dalton Trans.* **2017**, *46*, 8514–8523.

(41) Addison, A. W.; Rao, T. N. Synthesis, Structure, and Spectroscopic Properties of Copper(II) Compounds containing Nitrogen-Sulphur Donor Ligands ; the Crystal and Molecular Structure of Aqua[1,7-bis(N-methylbenzimidazol-2'-yl)-2,6-dithiaheptane]copper(II) Perchlorate. *J. Chem. Soc., Dalton Trans.* **1984**, 1349–1356.

(42) O'Keeffe, M.; Peskov, M. A.; Ramsden, S. J.; Yaghi, O. M. The Reticular Chemistry Structure Resource (RCSR) database of, and symbols for, crystal nets. *Accts. Chem. Res.* **2008**, *41*, 1782–1789.

(43) Fenton, H.; Tidmarsh, I. S.; Ward, M. D. Luminescent silver(I) coordination networks based on bis-(3,5-dimethylpyrazolyl)naphthalene ligands. *CrystEngComm* **2011**, *13*, 1432–1440.

(44) Gallego, M. L.; Cano, M.; Campo, J. A.; Heras, J. V.; Pinilla, E.; Torres, M. R. Supramolecular Arrays of Cationic Complexes Containing Pyrazole Ligands and Tetrafluoroborate, Trifluoromethanesulfonate, or Nitrate as Counterions. Crystal Structure of Bis(3,5–dimethyl–4–nitro–1H–pyrazole–κN^2)silver(1+) Nitrate ([Ag(Hpz^{NO2})$_2$](NO_3)). *Helv. Chim. Acta* **2005**, *88*, 2433–2440.

(45) Brese, N. E.; O'Keeffe, M. Bond-Valence Parameters for Solids. *Acta Crystallogr.* **1991**, *B47*, 192–197.

(46) Brown, I. D. *The Chemical Bond in Inorganic Chemistry: The Bond Valence Model*; Oxford University Press: Oxford, 2002.